Mississippi River channel response to the Bonnet Carré Spillway opening in the 2011 flood and its implications for the design and operation of river diversions

Mead A. Allison [a,*], Brian M. Vosburg [b], Michael T. Ramirez [a], Ehab A. Meselhe [c]

[a] University of Texas Institute for Geophysics, University of Texas, 10100 Burnet Road, (R2200) Austin, TX 78758-4445, USA
[b] Louisiana Coastal Protection and Restoration Authority, Baton Rouge, LA 70804-4027, USA
[c] The Water Institute of the Gulf, Baton Rouge, LA 70804, USA

ARTICLE INFO

SUMMARY

The large Mississippi River flood in 2011 was notable in the lowermost Louisiana, USA reach for requiring operation of several flood control structures to reduce stress on artificial levees: the largest diversion went through the gated Bonnet Carré Spillway, which was opened for 42 days in May and June. The removal of approximately 20% of the total flood discharge from the river provided an opportunity to examine the impact of large water diversion on the sediment transport capacity of large rivers.

Boat-based, acoustic and water and bed sampling surveys were conducted in the Mississippi River channel adjacent to the Spillway immediately prior to the opening of the structure, at full capacity, and immediately following (June 2011) and 1 year after (June 2012) closure. The surveys were designed to examine (1) elevation change of the channel bed due to scour or aggradation of sediment, and (2) suspended and bedload transport variability upriver and downriver of the Spillway. The results indicate that approximately 9.1 million tons of sand were deposited on the channel bed immediately downriver of the water exit pathway and extending at least 13 km downriver at a rapidly and progressively reducing magnitude per river kilometer. The surficial deposit was of finer grain size than the lateral sand bars in the channel upriver of the structure. We argue the deposit was largely delivered from suspension derived from the observed deflation of lateral bars upstream of the diversion point, rather than from sand arriving from the drainage basin. Approximately 69% of the 2011 flood deposit was removed from the 13 km downstream reach between June 2011 and June 2012. We conclude that the source of the channel deposit was the reduction in stream power, and, thus, in the sediment transport capacity of the Mississippi, associated with the water withdrawal. The re-entrainment of this material in the following flood year indicates the system rapidly re-establishes an equilibrium to pre-opening conditions. Future diversions in the river for coastal restoration will have to address this issue to maintain a deep draft navigation channel in the Mississippi River.

1. Introduction

Management of large rivers has often included the use of water diversions for a variety of purposes. Such diversions can have potentially deleterious effects downstream of the diversion point, either directly, through the reduction in water discharge in the main channel, or indirectly, through a reduction in the sediment transport capacity. Rarely, however, have these effects been quantified. For example, water diversions have been utilized in the Ganges River in India (e.g., Farakka Barrage) to divert water up to 1100 cubic meters per second (cms) into the Hoogly River distributary channel at lower river stages to maintain navigability and to flush accumulating river bottom fine sediment from the Port of Calcutta. Studies attributed to Farakka noted that reductions in

the water discharge in natural downstream distributary channels in adjacent Bangladesh have resulted in accelerating shoaling in these channels, and saline intrusion in adjacent deltaic wetlands (Mirza, 1998). In the Yellow (Huanghe) River in China, the diversion of water from the main channel in the lower drainage basin for irrigation to increase food production, has led to dry season water shortages further downstream in the basin (no-flow events) and channel shoaling ascribed to reduced transport capacity (Miao et al., 2011). In an extreme example, 85% of the flow of the Danube River was diverted into an artificial channel near the Hungarian–Slovakian border in 1996 to generate hydroelectric power, potentially impacting downstream wetlands and the drinking water supply (both surface and river-recharged groundwater aquifers (Smith et al., 2000)). Predicting the downstream impact of these structures prior to their construction, particularly on the sediment transport capacity of the system, is hindered by the limited availability of observational data to calibrate and validate numerical models of

the impact of diversions on river hydrodynamics and sediment dynamics.

In the lowermost Mississippi River in Louisiana (Fig. 1), water diversions are utilized for two purposes. Several large diversions (>5000 cms) have been constructed over the last approximately 75 years for flood control, specifically to divert water from the main channel to relieve pressure on the downstream, channel-lining artificial levees that protect cities such as Baton Rouge and New Orleans from flooding. Smaller structures (<212 cms) are utilized to divert freshwater to limit saline intrusion in adjacent deltaic wetlands and coastal water bodies, and to use for drinking water and industrial purposes. In addition, the most recent management plan for the coastal restoration of the degrading deltaic wetlands of the Mississippi Delta in Louisiana (LACPRA, 2012), calls for the construction of larger water and sediment channel diversions (up to 7080 cms at higher river stages) that can be utilized for wetland creation and restoration.

The large flood in May–June 2011 provided an opportunity to test channel response to a large-scale diversion from the Mississippi River associated with the use of the flood control structures, which operate only during the most extreme flood events. The primary objective of the present study is to (1) examine how the channel below the diversion responded to the removal of up to 8000 cms of water, and (2) document the sediment transport regime above and below the diversion during the period when the structure was opened to capacity. This observational dataset can help test the ability of multi-dimensional numerical simulations of channel hydrodynamics and the sediment transport that can better predict the future Mississippi River response to planned large diversions for delta restoration.

2. Study area

The lower Mississippi River in Louisiana divides into two distributary channels immediately upstream of the Tarbert Landing monitoring station at the Old River Control Structures (Fig. 1). The Old River outflow channel merges further downstream with the Red River near Simmesport, LA to form the Atchafalaya River distributary (Fig. 1). The main Mississippi distributary channel below Old River passes through lowland floodplain/alluvial valley to flow downriver of Baton Rouge, LA, and then across the Holocene-age

deltaic plain (Saucier, 1994) to the Gulf of Mexico (Fig. 1). Water movement through this lowermost Mississippi reach is coordinated by the U.S. Army Corps of Engineers through a flood control network that was designed to minimize the impact of large floods following the catastrophic 1927 Mississippi River flood. Within the Baton Rouge to New Orleans, LA reach that is the focus of this study, the river is lined with earthen levees located within 1 km of the channel banks and has stabilized banks (concrete mats in shallow water).

In large flood events when discharge at Red River Landing (e.g., below Old River Control immediately adjacent to the discharge measurement station at Tarbert Landing) reaches 1.25 million cfs (35,400 cms), additional water of up to the rated capacity of 250,000 cfs (7079 cms) is passed through the Bonnet Carré Spillway above New Orleans into Lake Pontchartrain (Fig. 1). Discharge above 1.5 million cfs (42,475 cms) is accommodated through the Morganza Spillway and West Atchafalaya Floodway upriver of Baton Rouge, and passing into the Atchafalaya Basin. The Bonnet Carré Spillway (RK 206; Fig. 1) was built between 1929 and 1936 as part of the post-1927 flood control system for the lower river. The structure is a 2134 m long concrete weir with 350 bays, each sealed with 20 timber "needles" that can be raised by a crane running along the weir top to allow river water to pass into an earthen leveled Spillway and flow into Lake Pontchartrain. Water only reaches the weir entrance bays at high discharges (>~24,900 cms), as the structure is fronted by a shallow forebay. Hence, it captures channel water from the uppermost water column. Opened on 10 occasions since 1937 (including 2011), detailed monitoring of water and suspended sediment discharge in the Spillway were conducted in the last three openings (1997, 2008, and 2011). The results of the first two events are compiled in Allison and Meselhe (2010). In 1997 when the structure was open for 23 days (maximum flow of 6600 cms), sampling was done at the Spillway, and at bridges crossing the Spillway 3.3 km and 8.8 km from the structure before the water enters Lake Pontchartrain. Allison and Meselhe (2010) demonstrated that a maximum of 340,000 tons/d (62% sand) of suspended sediment passed into the Spillway late in the rising limb of the flood (5985 cms diversion). Fallout of sediment (deposition in the Spillway) was rapid and weighted preferentially towards the more rapidly settling coarse fraction (sand). No river channel monitoring was conducted during either the 1997 or 2008 events.
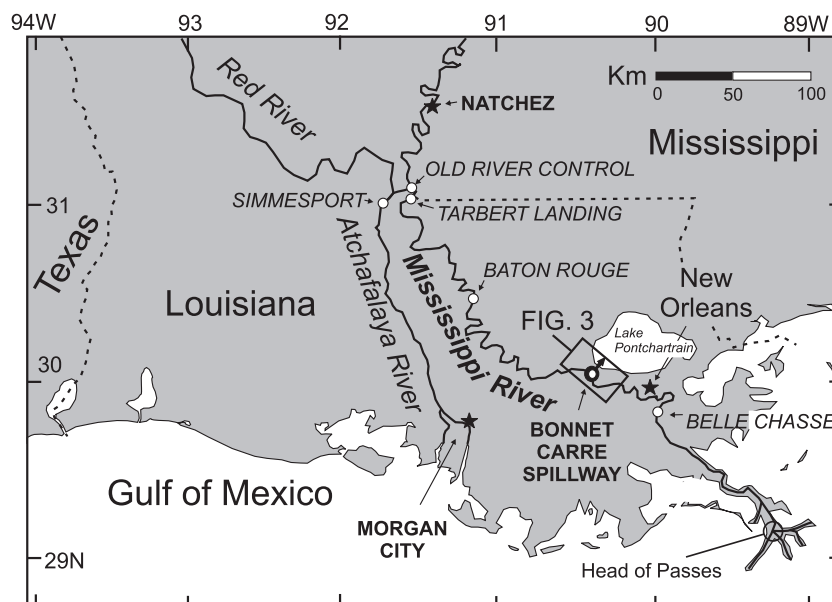

Fig. 1. Map of the study area showing the location of the Bonnet Carré Spillway and the limits of the larger map shown in Fig. 3.

3. The Mississippi River flood of 2011

In most years, the Mississippi hydrograph at the monitoring stations in Louisiana exhibits a large seasonal and inter-annual variability, with a high discharge (greater than approximately 28,300 cms) below Old River Control occurring between January and June, and typically with several individual peaks of 1–2 week duration. While the large Mississippi River flood of 2011 caused widespread flooding and property damage upriver of Old River Control, in Louisiana, a portion of the extreme flood was damped by passing water down the Atchafalaya pathway. The hydrograph at Tarbert Landing immediately below Old River Control (Fig. 1) shows a secondary peak in discharge (28,345 cms) on April 3, 2011, decreasing to 20,841 cms on April 18th, followed by the main peak that reached 45,845 cms during May 19–21, 2011. Even this damped maximum was above the previous peak water discharge (43,042 cms on April 11, 1945) recorded at this station since record keeping began in 1932.

The first gates (28 of 350) were opened at Bonnet Carré Spillway on May 9, 2011. The Spillway opening reached capacity (330 of 350 gates) on May 15th, and began closing gates on June 11th, and was fully closed on June 19th. The size of the flood also required the opening of the Morganza Spillway upriver of Baton Rouge for the first time since 1973. The first bays were opened on May 14, 2011, reaching the maximum water diverted (3228 cms, 17 of 125 bays) on May 18th. While the flood control protocol mandates a maximum flow of 250,000 cfs (7079 cms) through the Bonnet Carré Spillway during large floods, the measured flow (up to 8920 cms) at the Airline Highway bridge 3.3 km in the Spillway by the U.S. Geological Survey (Fig. 2) exceeded flood control design flow by 26% when operating at capacity after May 15th. Daily Mississippi River water discharges plotted in Fig. 2 show the values below the Morganza Spillway and above the Bonnet Carré Spillway (Baton Rouge monitoring station), as well as below Bonnet Carré Spillway (Belle Chasse station).

4. Methods

Three boat-based, acoustic and water and bed sampling surveys were carried out in the Mississippi River channel reach adjacent to the Bonnet Carré Spillway (Fig. 1) in May and June of 2011. They were timed to coincide with (1) the period immediately prior to the opening of the structure to divert flood water discharges (May 9–11th), (2) the period of maximum water discharge through the structure (May 21–22nd), and (3) the immediate post-closure period (June 21–25th). A fourth survey was conducted on June 12–14, 2012 to examine channel modifications one flood year after closure. The channel studies were divided into two components—mapping the channel bed bathymetric change induced by the Spillway opening, and examining the sediment transport (suspended and bed-load) in the channel above and below the structure while it was operating at full capacity (and again after closure). All four boat surveys were carried out on the 7 m vessel R/V Lake Itasca. Data were collected under the river discharge conditions recorded at the U.S. Geological Survey monitoring stations at Baton Rouge and Belle Chasse, Louisiana (Fig. 2). The Baton Rouge station is above the Bonnet Carré Spillway at river kilometer 372 (RK372) above the Head of Passes exit (RK0) of the Mississippi River (Fig. 1), while Belle Chasse is downriver (RK121) of the Bonnet Carré study area. Hence, when the Spillway is open, water discharges measured in the study area above the structure should more closely relate to Baton Rouge (off-set by the time for water to pass between the study sites), while those below should resemble Belle Chasse's level (Fig. 2).

Channel bed bathymetric data were collected during the pre-opening study (May 9–11, 2011) to build a basemap of the Mississippi River channel over a 19 river kilometer reach centered on the structure (Fig. 3). The data collection process was repeated during the post-opening studies and June 2012) to monitor the differences in the bed morphology over the period that Bonnet Carré Spillway was open (June 23–25, 2011), and channel morphology re-adjustment 1 year later (June 2012). Bathymetric data on all surveys were collected with a pole-mounted, Reson Seabat 7101 multi-beam (swath) bathymetry profiler (240 kHz; 511 depth beams; equal angle projection) and QPS (QINSy) software, which collects a swath width of up to 7.5 times the water depth. Basemap surveys were conducted with lines oriented in the along-river direction with limited swath overlap (~10%) to expedite mapping of this long river reach. Attitude data (heave, pitch, roll, and yaw) were collected at 1 ms intervals with a gyroscope inertial guidance system (Applanix, Inc.), mounted inside the vessel hull. Dual antenna
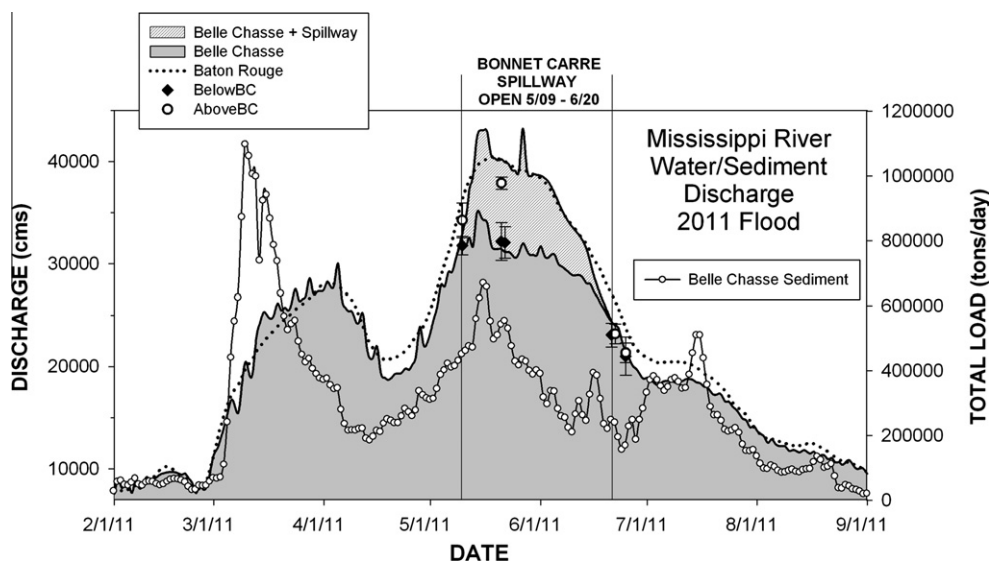

Fig. 2. Water and sediment discharge in the Mississippi River in Louisiana associated with the 2011 flood event. Shaded areas represent the measured daily water discharge at the USGS station at Belle Chasse alone (darker shade), and the water discharge measured in the Spillway at the Airline Highway bridge by USGS (lighter shade). The latter agrees well with daily water discharge at the USGS station upriver of the Spillway (Baton Rouge, dotted line). Point data represents ADCP transects made to measure water discharge upriver (AboveBC) and downriver (BelowBC) of the Spillway. Error bars were developed from multiple transects done in immediate succession. Calculated daily sediment load (from a calibrated OBS turbidity measurement at the USGS Belle Chasse station) downriver of the Spillway is also shown.
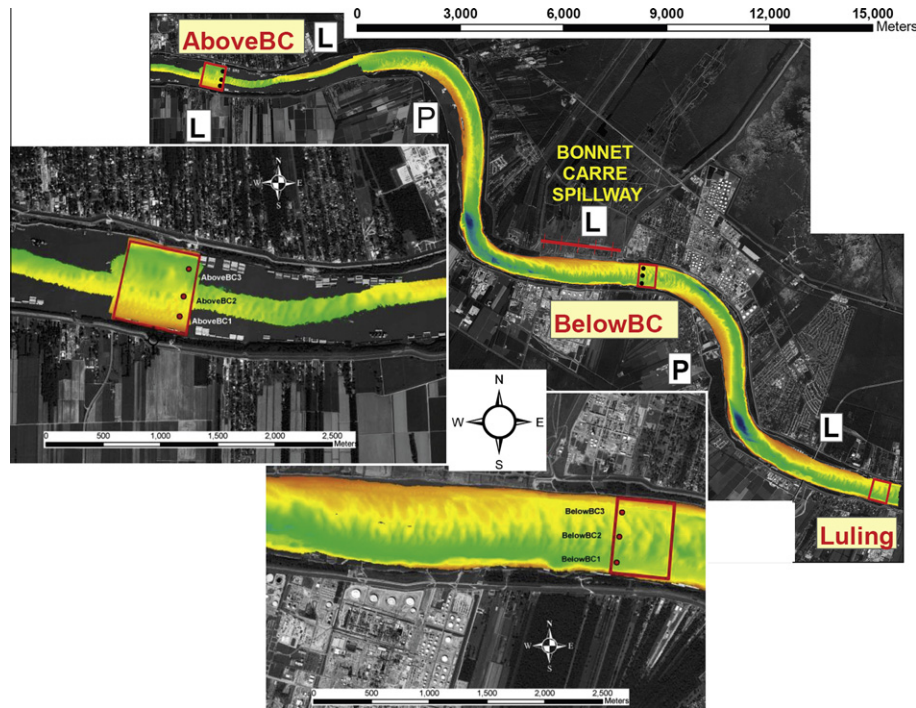
Fig. 3. Large-scale map of the study area showing the channel bathymetry (collected mainly during the post-opening Spillway survey), the location of the Spillway, and detailed study sites for the bedload and suspended load measurements. The "L" refers to the location of lateral bars, and the "P" indicates the location of point bars described in the text.

differential GPS provided position, heading, and velocity data, which were integrated with measurements of ship attitude using Applanix POS/MV hardware. Common survey values for the attitude, heading, position, and velocity error were ~0.025°, 0.018°, 0.3 m, and 0.04 m/s, respectively. Vertical resolution (theoretical) for the multibeam instrument, as estimated by the manufacturer, is approximately 1.5 cm.

After data collection, raw files were converted to industry standard XTF format and were imported into CARIS© HIPS 7.1 software for post-processing. Post-processing includes removal of multiples, other noise, and navigation drop-outs. Data were then corrected for elevation of the water surface (combination of river stage and tidal phase), using a CARIS interpolation of hourly U.S. Army Corps of Engineers (USACE) water level (stage) gage data reported in 0.01 foot (0.3 cm) precision, and referenced to NGVD sea level at Reserve (RK223.2), Bonnet Carré (RK204.2), and Carrollton (RK165.4). Sound velocity correction was applied at the standard 1500 m/s for freshwater. Motion sensor and navigation data were then merged and channel bathymetry grids of 1×1 m cell size and 5×5 m cell size were created in HIPS and exported to ArcView software for elevation differencing.

Multibeam bathymetric data were collected to calculate the bedload transport rates in the channel using a modified version of the three-dimensional dune migration survey and post-processing methods developed by Nittrouer et al. (2008). Survey data were collected at AboveBC (above the Bonnet Carré Spillway at RK221), BelowBC (just below the Bonnet Carré Spillway at RK203) and Luling (RK196) during the Spillway operation at capacity (May 21–22nd) and post-opening (June 22–23rd) (Fig. 3). Each grid area survey consisted of two bank-to-bank data sets of an approximately 500 m long river reach collected within 24 h of one another and requiring about 1.5 h of survey time for the grid's coverage from bank-to-bank. During the May surveys of maximum dune celerity, repeat surveys were collected only 6–8 h apart. Bedload bathymetry transects were conducted with at least 30% swath overlap and repeated surveys followed a similar line order and direction.

Initial post-processing and the export of 1 m cell size grids followed the methods for the basemap survey. Visual identification of crest locations confirmed that dunes had migrated less than one wavelength (10–200 m depending on dune size) between surveys (a prerequisite of the survey). A set of bedform field polygons was outlined for the independent calculation of dune migration volumes, corresponding to areas of similar bedform wavelength. These varied in downriver width from between survey sites and cruises due to the effect mentioned above, and in river width as the bedform field changed dimensions. The volume of sand deposited for each polygon was calculated by assuming a sediment porosity of 35% and a grain density of 2650 kg/m³. These values were converted to final bed material flux measurements (q_s in m³/s) for each cross-sectional polygon, and were then summed cross-channel to derive final bedform translational fluxes (Q_s in mass per unit time) for that river grid area. Two results were produced for each measurement and they corresponded to the area eroded (up current side of the migrating dunes) and accreted (down current side). Nittrouer et al. (2008) provides a more thorough explanation of the methods and equations utilized in this bedload study.

The AboveBC and BelowBC study areas were also examined for water and suspended sediment discharge in surveys when the Spillway was open (May 21–22nd and after its closure (June 22–23nd). Cross-sectional water discharge was measured with a pole-mounted, 600 kHz RD Instruments Workhorse Monitor acoustic doppler current profiler (ADCP) along a series of transects inside the bedload study grid area (Fig. 3). WinRiver© software (RD Instruments) was utilized to collect four bank-to-bank transects in rapid succession—two in each direction. The ADCP cross-sectional data were collected at additional points outside the study grids and during the pre-opening survey on May 9–11, 2011 (Fig. 3). The WinRiver software utilized for data collection integrates across the channel by extrapolating the areas of the channel cross-section not directly measured. For example, water above the sensor, the near bottom, and right and left banks were too shallow to survey.

The depth of sensor is fixed (40 cm), and the distance to the banks are entered manually for each survey. No water and suspended sediment discharge data were collected at the Luling site.

Three stations were established along the ADCP cross-sections at AboveBC and BelowBC (Fig. 3) and corresponded to the top and face of the lateral bar, as well as the channel thalweg. At each of the six stations from the May and June studies, one liter isokinetic water samples were collected with a 91 kg, P-63 point integrative sampler at the surface, 0.3, 0.5, 0.7 and 0.9 total water depth. Synchronous with the 15–30 min period during which the isokinetic samples were being collected at each station, stationary ADCP measurements were carried out to provide time-series averages of site currents using the multibeam positioning system to remain on site within about 1 boat length. Water column profiles were also conducted immediately before or after the P-6 sampling with a Seabird SBE-11 CTD (conductivity/temperature/depth) profiler that measured these parameters.

Suspended sediment loads during the maximum Spillway opening and post-closure were calculated from the water discharge results presented in Table 1 and isokinetic point sampler data in accordance with the methods outlined in Edwards and Glysson (1988). Each river cross-section was divided into subsections that each have a vertical sampler station at the mid-point of the subsection. In each cross-section, the mean concentration of sediment was calculated as a depth average of the P-63 isokinetic point samples. The WinRiver software was then used to calculate the portion of the total ADCP cross-sectional water discharge contained within that subsection from surface to bottom. This was done for each of the four repeat cross-sections and the average was utilized for the suspended sediment load calculations.

A 5 cm path length transmissometer and a Campbell Scientific OBS-3 optical backscatterance sensor were mounted on the CTD and were time-synchronized with the CTD to sample at a 1 Hz frequency in the down and upcast. A Sequoia Scientific Laser In Situ Scattering and Transmissometry (LISST) sensor was also attached to the CTD profiler frame and operated during each cast. This LISST 100-X model, type C, measures particle size over a size range of 2.5 µm to 500 µm. This unit was machined to a 1 cm optical gap (80% path reduction) to compensate for the relatively high turbidities in the Mississippi River, and operated by magnetic switch to begin sampling at a 1 Hz rate at the onset of the cast. Each 1 Hz sample was an average of 10 discrete samples. Daily surface water samples were collected and settled for 1 day prior to running a

background (zscat), that was applied to each day's LISST data. Each of the six sampling sites was also bed sampled on both surveys with a Shipek grab sampler.

In the laboratory, isokinetic water samples were sieved through a 63 µm sieve to separate the sand fraction and vacuum-filtered through pre-weighed 0.2 µm polycarbonate filters to concentrate sediment for drying and weighing. A graduated cylinder was utilized to determine the water sample size (in ml) of the filtered sample, and then the total suspended concentration (in mg/l) of those results, and the summation of mud and sand concentrations. The sand fraction for each sample was further analyzed for granulometry at 1/10 phi size intervals using a Retsch Technologies Camsizer. Several surface samples contained too little sand for analysis.

The grain size of bottom grab samples was determined by wet sieving through stacked 2 mm and 63 µm sieves to concentrate the gravel and sand fractions, respectively. Sand and organic fractions were dried in an oven at 60 °C and weighed to determine total weights. The dried fractions were then heat treated in a muffle furnace at 550 °C for at least 12 h to remove organics, and reweighed do determine sand and organic content. All gravel and organic fraction materials were observed to be a woody material. Sand fractions from the bottom grabs were further analyzed for detailed size fractions using a Femto automated settling column. The sample mass was too small to utilize this method for the isokinetic samples.

5. Results

5.1. Channel morphology and bed character

The multibeam bathymetry (basemap) survey shown in Fig. 3 represents the more extensive (20 river km), bank-to-bank coverage of the post-opening (June 2011) data collection. It also includes the upriver single line survey that was carried out further upriver in the pre-opening (May) survey, and the AboveBC bedload grid obtained in the post-opening survey—these data allow maximum coverage for defining channel morphology. The surveyed channel reach is most broadly defined by six, 3–5 km long, bank-attached lateral bars and point bars (defined here as a lateral bar at the inside of a highly sinuous meander bend). These bars alternate from east to west bank, and include a lateral bar immediately adjacent to the forebay of the Spillway (Fig. 3). The thalweg alternates from the east to west side of the channel with the bar morphology, and

Table 1
Cross-sectional water discharges and suspended sediment loads measured at Bonnet Carré survey sites.

Survey grid[e]	Study dates (h)[f]	Q_w at Baton Rouge (m³/s)	Q_w at Belle Chasse (m³/s)	Mean measured Q_w (m³/s)[a]	Sand (tons/d)[d]	Mud (tons/d)[c]
AboveBC RK208.4	05/10/11 1758–1810	36,415	31,998	34,258 ± 1692		
BC RK206.0[b]	05/10/11 1820–1832	36,415	31,998	31,870 ± 1758		
BelowBC	05/10/11 1842–1854	36,415	31,998	31,791 ± 912		
AboveBC	05/21/11 1234–1307	40,182	31,432	37,878 ± 601	321,850	304,951
AboveBC RK210.0	05/21/11 1758–1810	40,182	31,432	39,077 ± 455		
BC 206.0[b]	05/21/11 1825–1837	40,182	31,432	32,706 ± 1419		
BelowBC	05/21/11 1848–1900	40,182	31,432	32,177 ± 1845		
BelowBC	05/22/11 1324–1346	40,012	31,149	32,088 ± 1542	173,475	250,533
AboveBC RK208.4	05/22/11 1552–1614	40,012	31,149	37,918 ± 707		
BelowBC	06/21/11 1454–1515	27,051	24,381	23,080 ± 1155	80,044	125,944
AboveBC	06/22/11 1537–1558	26,388	24,013	23,188 ± 965	31,757	119,609
AboveBC	06/25/11 1131–1143	23,795	21,521	21,347 ± 963		
BelowBC	06/25/11 1207–1219	23,795	21,521	21,004 ± 1862		

[a] Data was collected with the 600 kHz ADCP, ±reflects one standard deviation.
[b] Transect normal to Bonnet Carré spillway structure.
[c] Refers to the fraction smaller than 63 µm that passed through the sieve and was collected onto 0.2 µm filters.
[d] Refers to the fraction larger than 63 µm collected on a sieve.
[e] Above BC = Bonnet Carré survey area above Bonnet Carré Spillway at RK221.3, Below BC = Bonnet Carré survey area below Bonnet Carré Spillway at RK204.2, BC# = Bonnet Carré survey at #equivalent to river kilometer.
[f] Times for these surveys are in Greenwich Mean (GMT).

is typically 25–35 m deep at a point opposite the lateral bars, reaching 40–45 m deep opposite the point bars in the meander bends. The thalweg in the meander bends, and to a lesser extent opposite the lateral bars, and the steep channel walls on the opposite bank show evidence (e.g., flutes, terraces, rip-up scars) of the exposure of relict, fluvio-deltaic substratum previously observed in the channel below New Orleans (Nittrouer et al., 2011a).

The bars themselves are covered by dunes that were present throughout the flood and typically increase in size (amplitude and wavelength) from the bar top to bar face, except in flat, shallow, near-bank areas (less than approximately 10 m water depth). Dunes range from 1 to 3 m high and 20 to 30 m in wavelength on the bar tops, reaching 4–6 m high and 50–200 m in wavelength on the bar face in 25–35 m of water. The largest bedforms at the downriver end of each bar migrate across channel and climb the steep bar face of the next lateral bar on the opposing bank. On long bars, such as the ∼5 km long one at Luling (Fig. 3), dune wavelength and height was observed to increase along-bar (e.g., downriver). In general, the pre-opening survey, which was done at a much higher water discharge, revealed larger dunes in equivalent areas. Even larger dunes were observed in the limited multibeam data surveyed for bedload transport measurements (see Section 5.3) during the period when the Spillway was open and water discharge was at a maximum.

The six bottom grab stations on the bars (see Fig. 3 and Table 2 for locations) at AboveBC and BelowBC that were sampled during the period when the Spillway was open, and again post-opening, indicate that the surficial lateral bar deposits are composed of 96–100% sand. Table 3 shows size statistics of the sand fraction from these samples. All samples can be classified as either fine (125–250 μm) or medium (250–500 μm) sand. The three sample sites on each bar were selected to correspond with areas of shallow "bar top" (AboveBC1, BelowBC3), steeper "bar face" with the largest bedforms (AboveBC2, BelowBC2), and "thalweg" (AboveBC3, BelowBC1). On the AboveBC bar, samples from the bar top and bar face were finer in the post-opening survey compared to the sampling during the Spillway opening. The surficial thalweg deposits, which had sand cover over the relict substratum at both sites, were coarser at the post-opening AboveBC site. Relative to AboveBC, all three stations at BelowBC show an insignificant difference between the two sample periods, with much finer sand on the bar top and bar face than at the AboveBC site (Table 3).

5.2. Channel sand storage

The 1 m grid of the pre- and June 2011 post-opening basemap multibeam surveys corrected to NGVD elevation using river stage

gauge data (see methods) were differenced (Fig. 4b) to depict any shallowing (bed accretion) or deepening (bed scour) of the channel bed. The same was then done to the June 2012 survey to allow for continued morphological change to be examined after the early 2012 flood (Fig. 4c). Four patterns are immediately apparent in Fig. 4b. The first is an alternating erosion and accretion in the downriver direction on approximately 100 m length scales resulting from the migration of individual dunes and the offset of crests and troughs between surveys. The second pattern shows that the areas with the largest elevation change, which are mainly confined to the central channel, alternate in bank proximity (east or west) with the bar morphology. Near bank areas tend to display elevation changes of 1 m or less. This central "belt" of elevation change mainly corresponds with the steep bar faces of the largest bedforms and follows their thalweg crossings at the downriver end of each lateral bar. The third pattern is a 3–4 km long (downriver) zone of mainly accretion (up to 7 m of elevation change) beginning adjacent to the downriver half of the Bonnet Carré Spillway's forebay (Fig. 4b). The final pattern is a restricted (∼0.5 km long), but large magnitude (up to 7 m of elevation change), pattern of erosion of bar tops and accretion at the downstream edge of the two bars (1 lateral, 1 point) above the Spillway. This downstream edge accretion is also observed at the point bar downriver of the Spillway (Fig. 3). The accretion is found in deep thalweg areas of 35–40 m water depth (see Fig. 4b).

To quantify the magnitude in volume and mass of the observed accretion and erosion, the surveyed channel was divided into nine segments generally located where a change from accretion to erosion was observed from the patterns mentioned above and at lateral bar bank crossings. These segments are labeled A–I in Fig. 4a. The total volume change in that reach was quantified (m^3) and converted into sediment mass in Table 2 using a volume to mass ratio of 1361.6 kg/m^3, which is the standard conversion for dredged volume calculations utilized by the U.S. Army Corps of Engineers in Louisiana.

The results of this analysis indicate that the river channel upriver of the Spillway (segments A–D in Fig. 4b) underwent alternating bed erosion (segments A and C) and accretion (B and D) that was associated with the deflation of the bar surfaces (not as apparent a pattern as the four mentioned above), as well as the deposition of sand on the downstream edge of the bars. This cannot be stated definitively since bank-to-bank coverage was not acquired in this reach. In front of the forebay entrance to the Spillway, the upriver half of the channel experienced net erosion, including the lip of the forebay (E), while the downriver half experienced massive accretion (segment F). This accretion continued with the progressive decrease in magnitude below the Spillway entrance (F to

Table 2
Bathymetric change of river segments (locations in Fig. 3) observed between the pre- and post-opening surveys at Bonnet Carré Spillway.

Segment	Length in river (km)	Polygon area (10^6 m^2)[b]	May 2011 to June 2011[a]			June 2011 to June 2012[a]			May 2011 to June 2012[a]		
			Polygon average change (m)	Polygon volume change (10^6 m^3)	Polygon mass change (10^6 T)	Polygon average change (m)	Polygon volume change (10^6 m^3)	Polygon mass change (10^6 T)	Polygon average change (m)	Polygon volume change (10^6 m^3)	Polygon mass change (10^6 T)
A	0.56	0.18	−0.95	−0.90	0.12	0.35	0.06	0.08	0.32	0.03	0.03
B	2.09	0.63	1.48	3.75	0.51	−1.17	−0.74	−1.01	0.30	0.08	0.11
C	1.93	0.71	−1.36	−3.71	−0.51	1.72	1.21	1.65	0.48	0.13	0.17
D	3.22	1.23	1.01	12.54	1.71	−0.39	−0.47	−0.64	0.76	0.87	1.18
E	2.25	1.35	−0.06	−0.89	−0.12	−0.27	−0.36	−0.49	−0.31	−0.42	−0.58
F	3.70	1.67	2.87	47.91	6.52	−2.42	−4.03	−5.48	0.42	0.70	0.96
G	2.41	0.93	1.11	10.30	1.40	0.89	0.83	1.13	1.97	1.83	2.49
H	3.54	1.43	0.34	4.97	0.68	0.07	0.09	0.13	0.32	0.46	0.62
I	4.62	1.91	0.17	3.64	0.50	−0.81	−1.54	−2.10	−0.68	−1.31	−1.78

[a] Positive numbers refer to bed shallowing (accretion) between the pre- and post-opening surveys and negative numbers indicate bed deepening (erosion).
[b] Polygon areas are based on bank-to-bank coverages collected in June 2011 and June 2012. In segments A–D in May 2011, a reduced polygon area was utilized to calculate average change (in m) to reflect the reduced multibeam coverage in this dataset.

Table 3
Sand grain size statistics of bottom grabs at AboveBC and BelowBC.

Station name and depth (m)	Collection dates	Latitude and longitude (°)	Mean (µm)[b]	Std. dev. (µm)	% Coarse sand[c]	% Med. sand	% Fine sand	D_{10} (µm)[a]	D_{50} (µm)	D_{90} (µm)
AboveBC1	05/21/11	30.04638	258.6	64.07	0.2	54.9	45.0	209.9	255.5	309.4
(19.2)	06/23/11	−90.54908	225.3	73.52	0.3	23.5	75.1	172.3	221.2	275.1
AboveBC2	05/21/11	30.04794	339.2	73.10	0.8	92.1	7.0	261.9	337.5	414.4
(22.9)	06/23/11	−90.54869	311.7	87.49	0.4	73.6	25.5	210.2	320.6	400.5
AboveBC3	05/21/11	30.05008	229.3	47.36	0.1	22.0	77.9	187.5	229.2	281.4
(28.7)	06/23/11	−90.54817	260.6	67.62	0.2	52.9	46.6	214.3	252.4	312.8
BelowBC1	05/22/11	29.99204	344.6	91.28	2.7	86.1	11.1	245.6	343.8	437.8
(25.9)	06/21/11	−90.42309	438.0	113.3	0.6	85.2	10.0	342.0	428.3	532.0
BelowBC2	05/22/11	29.99406	192.0	28.98	0	1.5	97.4	164.8	191.5	218.8
(21.6)	06/21/11	−90.42279	199.2	47.16	0.2	3.4	95.3	172.7	196.8	223.7
BelowBC3	05/22/11	29.99597	171.1	59.25	0	0.2	96.9	144.1	169.6	194.5
(21.3)	06/21/11	−90.42249	181.8	64.97	0.2	1.4	95.4	150.2	179.4	210.0

[a] D_{10} is the 10th percentile of cumulative size frequency, D_{50} is the 50th percentile (median), and D_{90} is the 90th percentile.
[b] Mean and standard deviation were calculated using the arithmetic method of moments.
[c] Coarse sand is the 500–1000 µm fraction, medium is the 250–500 µm, fine is the 125–250 µm. The remaining percentage not listed is very fine sand (62.5–125 µm).
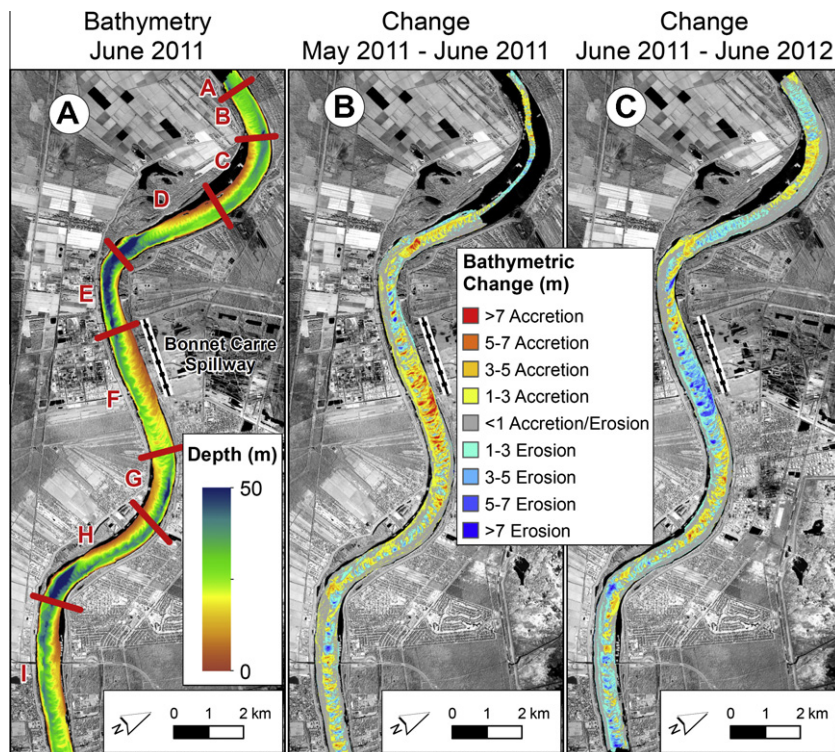

Fig. 4. (A) Bathymetric map of the studied river channel reach collected in June 2011. The bathymetric map shows the limits of the river reach segments defined to create volume change calculations in Table 2. Segments A and I are to the upriver and downriver limit of the overlapping data, respectively. (B) Bathymetric change map displaying the elevation change between the pre- and post-Bonnet Carré Spillway multibeam bathymetric surveys in May and June of 2011. (C) Bathymetric change map displaying the elevation change between the immediate post-closure survey in June 2011 and the bathymetry collected after the 2012 flood year (June 2012).

I). The total accretion below the Spillway in the channel was 6.68×10^6 m^3, which converts to 9.1 million tons (Table 2).

Between the June 2011 and June 2012 surveys (Fig. 4c), the river had three moderate flood peaks of 22,650–24,640 cms in December 2011 to April 2012, as recorded at the USGS Baton Rouge station. Upriver of the Spillway, the pattern of lateral and point bar elevation change was reversed compared to the earlier comparison survey, with accretion of the bar top and partial removal of the deposits that accreted at the downstream edges. Much of the accretion downriver of the Spillway (integrating segments F to I) was removed (4.65×10^6 m^3 or 6.3 million tons; Table 2) between June 2011 and June 2012 (Fig. 4c).

5.3. Bedload flux measurements

Bedload (bedform) flux rate results for each site and study are shown in Table 4 and in Fig. 5. The two results produced for each measurement, which correspond to the area eroded (up current side of the migrating dunes) and accreted (down current side). In previous work (Nittrouer et al., 2008; Allison and Meselhe, 2010), the two results have shown close correspondence. In the Bonnet Carré bedload data, however, there are significant differences. As shown in Fig. 5, when the Spillway was open at capacity (i.e., maximum river discharge), accretion was less than erosion at all three study sites; decreasing in difference from 69% of the erosion at

Table 4
Bedload (bedform) mass flux rates at AboveBC, BelowBC and Luling grids during and after the opening of the Spillway.

Survey grid[b]	Study dates (h)[c]	River (km)[d]	Polygon# and channel width (m)	Polygon flux per unit width (q_s in m²/s)	Q_s (accretion) in tons/d[a]	Q_s (erosion) in tons/d
AboveBC	1610–1725 May 21	137.7	P1(266)	1.25E−03	85,240	120,687
(Open)	2118–2228 May 21		P2(146)	1.07E−03		
			P3(121)	4.28E−04		
BelowBC	1731–1821 May 22	126.7	P1(340)	1.76E−03	120,898	148,809
(Open)	2138–2220 May 22		P2(92)	4.95E−04		
			P3(50)	9.51E−05		
Luling	1617–1707 May 22		P1(287)	1.72E−03		
(Open)	2240–2303 May 22	120.3	P2(56)	2.52E−03	101,109	116,735
			P3(36)	4.89E−05		
AboveBC	1906–2015 June 22	137.7	P1(261)	2.11E−04	20,874	14,080
(Closed)	1700–1758 June 23		P2(224)	2.83E−05		
BelowBC	1829–1941 June 21	126.7	P1(440)	7.12E−04	68,269	75,021
(Closed)	1724–1818 June 22		P2(62)	2.26E−04		
			P3(44)	8.25E−06		
Luling	2256–2337 June 21		P1(74)	1.19E−04		
(Closed)	1612–1651 June 22	120.3	P2(340)	7.69E−04	62,095	61,936

[a] Q_s is channel width integrated mass flux in metric tons/d. "accretion" refers to the calculations of the downstream growth of dunes, and "erosion" refers to upstream deflation associated with downriver migration of the dunes.
[b] Above BC = Bonnet Carré survey area above Bonnet Carré Spillway structure, Below BC = Bonnet Carré survey area below Bonnet Carré Spillway structure, Luling = Bonnet Carré survey area below Luling Bridge.
[c] Times for these surveys are in Greenwich Mean (GMT).
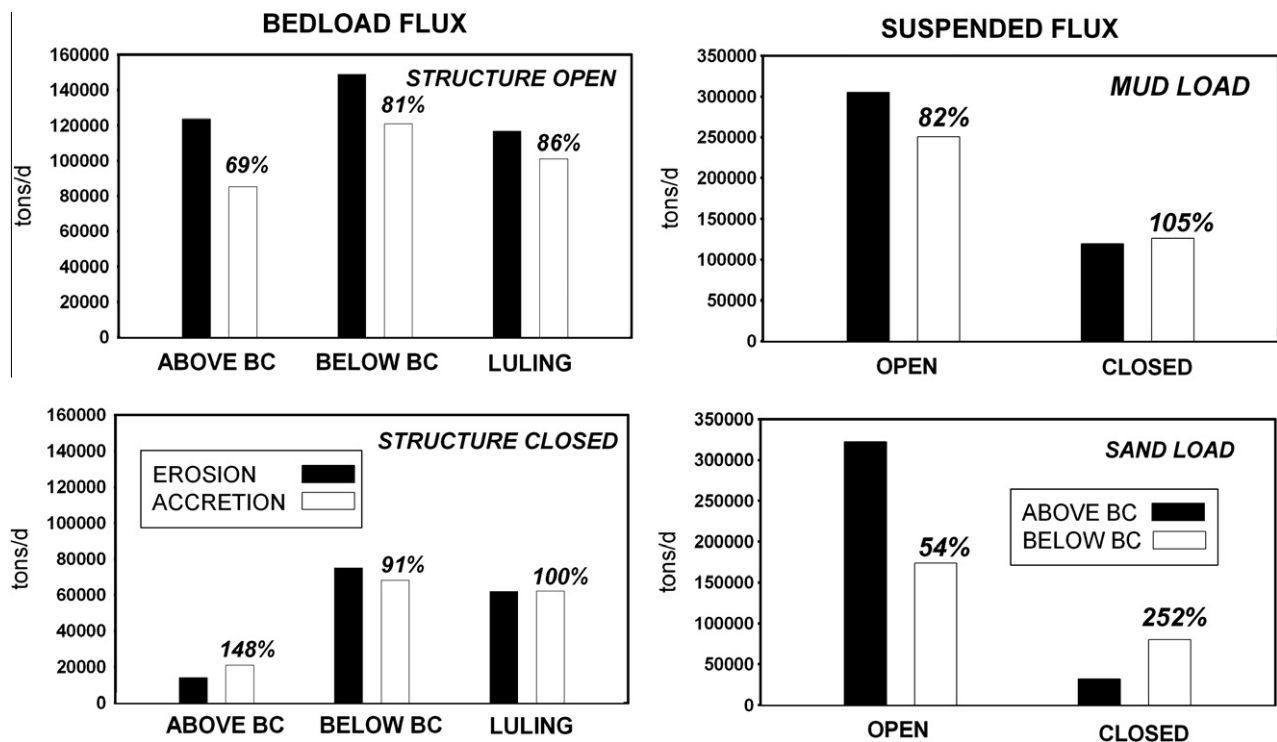[d] River mile of the center of the survey grid reach.

Fig. 5. Histograms of bedload and suspended load (divided into mud and sand fractions) fluxes at the three study sites (AboveBC, BelowBC and Luling; Fig. 3) while the Spillway was operating at capacity ("open", May 21–22, 2011) and post-closure ("closed", June 21–22, 2011). Bedload flux is expressed as the accretion on the downstream edge of the dunes and erosion of the upstream edge.

AboveBC, to 86% at Luling. The highest average of the bedload flux (mean of accretion and erosion values) was at BelowBC, despite the reduction of water (due to the Spillway) at AboveBC. In the falling water discharge post-closure survey, the average bedload flux was reduced at all three sites relative to the earlier survey. Again, the BelowBC values were the greatest. The accretion flux was still lower at BelowBC (91% of erosion) but was higher at AboveBC (14%). The accretion magnitude at Luling was the same as erosion (Fig. 5).

5.4. Water and suspended load flux measurements

Cross-sectional water discharge was collected during each 2011 survey at AboveBC and BelowBC help calculate suspended sediment load along those cross-sections. Measured daily water discharges are shown in Table 1 and Fig. 2, along with the daily USGS station averages at Belle Chasse (below Bonnet Carré) and Baton Rouge (above Bonnet Carré). The results shown represent

averages and standard deviations of these four replicate ADCP crossings.

Measured water discharge at the sites above (AboveBC) and below (BelowBC) the Spillway in the early opening phase (May 10, 2011) when discharge through the Spillway was only about 3500 cms (measured by the USGS at the Airline Highway bridge (and shown in Fig. 4a)) ranged from 31,791 to 34,258 cms, while the discharges at Baton Rouge and Belle Chasse were 36,415 and 31,998, respectively. Water discharge through the Spillway during the May 21–22nd surveys was at a maximum (8700 cms), and the discharges at the sites above and below the Spillway reflected this water loss: AboveBC was measured at 37,898–39,077 cms and BelowBC at 32,088–32,177 cms (Table 1). After Spillway closure during the falling discharge phase, measured discharge was
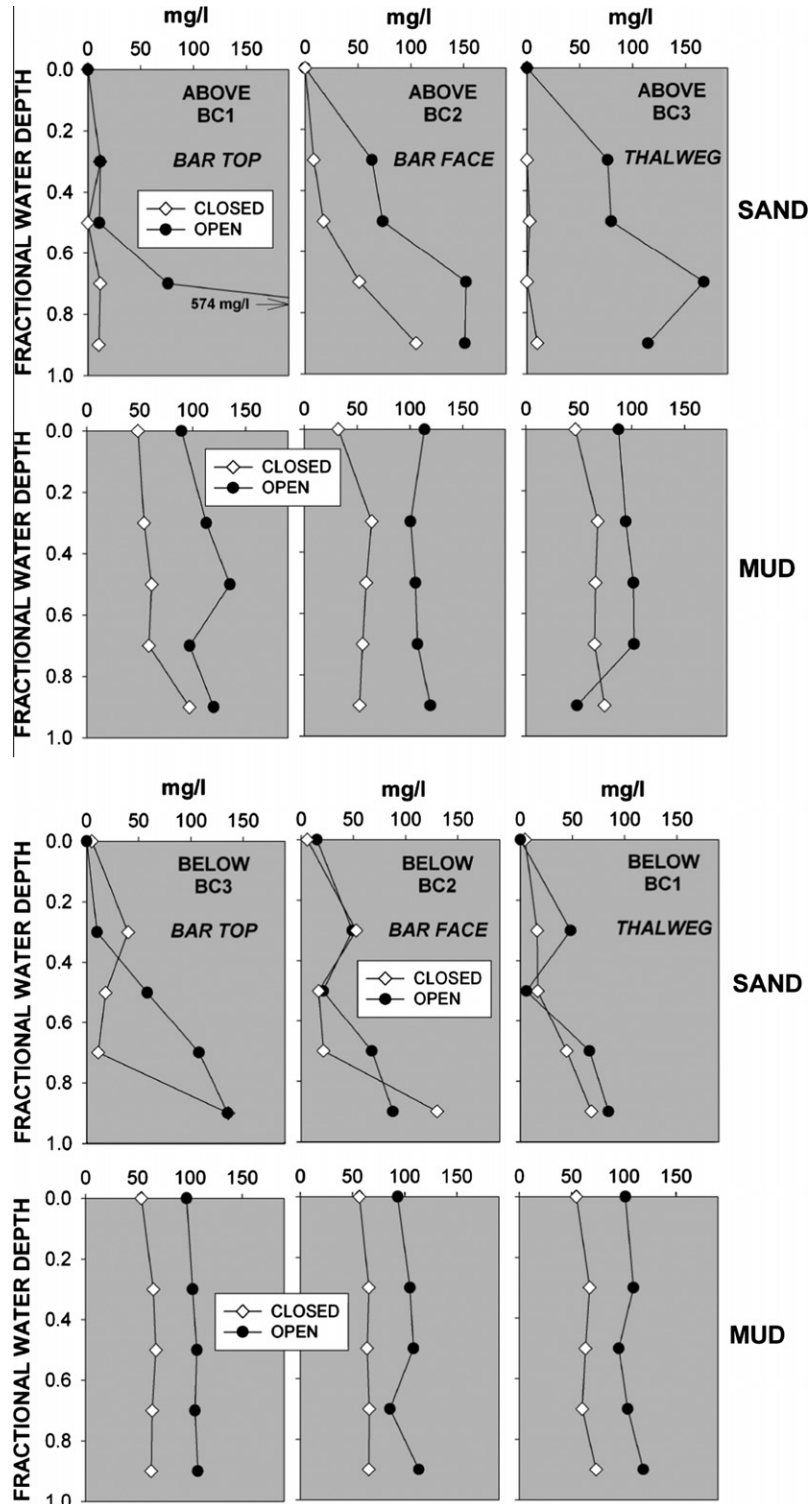

Fig. 6. Suspended load concentrations (mud and sand) at the three study sites at AboveBC (upper) and BelowBC (lower) (Fig. 3) measured using the point-integrative sampler while the Spillway was operating at capacity ("open", May 21–22, 2011) and post-closure ("closed", June 21–22, 2011).

approximately 23,100 cms on June 21, 2011, to about 21,180 cms on June 25th.

Suspended sediment loads at the AboveBC and BelowBC transects for the maximum opening survey (May 21–22nd) and post-closure survey (June 21–22nd) are shown in Table 1 and Fig. 5. Suspended mud flux was reduced at BelowBC to 82% of the measured flux above the Spillway when it was open to capacity. Suspended sand flux was reduced to an even greater degree (54% of AboveBC). After the Spillway closure in June 2011, measured mud fluxes were approximately equivalent above and below the Spillway, and were reduced by a factor of two relative to the May 2011 surveys (Fig. 5). Sand fluxes, although reduced by a factor of two or more relative to the May surveys, show a reversal in downriver trend, with the BelowBC values being 252% of those at AboveBC.

In Fig. 6, suspended sand loads at the measurement sites are compared to the nearest USGS monitoring station data above (Baton Rouge) and below (Belle Chasse) during the flood. Ratings curve sand load data at Baton Rouge and Belle Chasse were calibrated (not shown) with monthly, boat-based, USGS cross-sectional measurements using a 130 kg, D99-series depth integrated sampler that Allison et al. (2012) used for flood years 2008–2010. This sand ratings curve was adjusted for the additional data collection in 2011, which were unavailable in the previous work. The ratings curve and D99 measurements are shown for both USGS stations in Fig. 6. They demonstrate that the relatively limited number of measurements made in the present study are consistent with those calculated and measured at the USGS stations above and below the Spillway.

A total (sand + mud) daily suspended load is shown in Fig. 2 for the USGS station at Belle Chasse. This total load is based on calibrated (D99 sampling cross-sectional transects) optical turbidity (NTU) measurements found in Allison et al. (2012). Again, the value is adjusted (recalibration not shown) to include 2011 data.

Totaling the mud and sand load (Table 1) for the BelowBC station when the Spillway was open to capacity (May 21st) yields 424,005 tons/d compared to the calibrated turbidity value of 543,608 tons/d on that date. After the Spillway closure, the measurements at BelowBC on June 21st (205,988 tons/d) are closer to the USGS Belle Chasse value of 249,339 tons/d than the measurements at AboveBC June 22nd (151,366 tons/d) versus 240,937 at USGS Belle Chasse.

The laboratory breakdown of sand size classes in the isokinetic (suspended) data from the six stations shows a general overall trend coarsening (mean size) approaching the river bed. This trend is particularly apparent in the two bar face stations (AboveBC2 and BelowBC2) with the largest dunes. Fig. 7 shows concentration to frequency plots for these two stations during the period of maximum Spillway operation and after closure. At AboveBC2, the mode of the frequency distribution coarsens with depth from about 180 to 230 μm as the overall sand concentration increases. This coarsening is also true in the lower sand concentration post-closure samples. The mode of the suspended sand grain size is considerably finer than that of the underlying bed (grab sample median of about 330 μm) both when the Spillway was open and closed (Fig. 7). At BelowBC2, the same trends with depth are apparent and the mode of the suspended sand is similar to AboveBC. Unlike AboveBC, the underlying bed is much finer (median about 195 μm) and of equivalent grain size to the suspended sand mode. The results from the optical measurements (total volume concentration from the LISST and optical backscatterance from the OBS-3) on the wire-deployed profiler are not shown because of the limited isokinetic data available to calibrate them to total suspended sediment concentration. However, both instruments confirm the isokinetic results that indicate the increased turbidity/concentration with increasing water depth during and after the Spillway's opening.
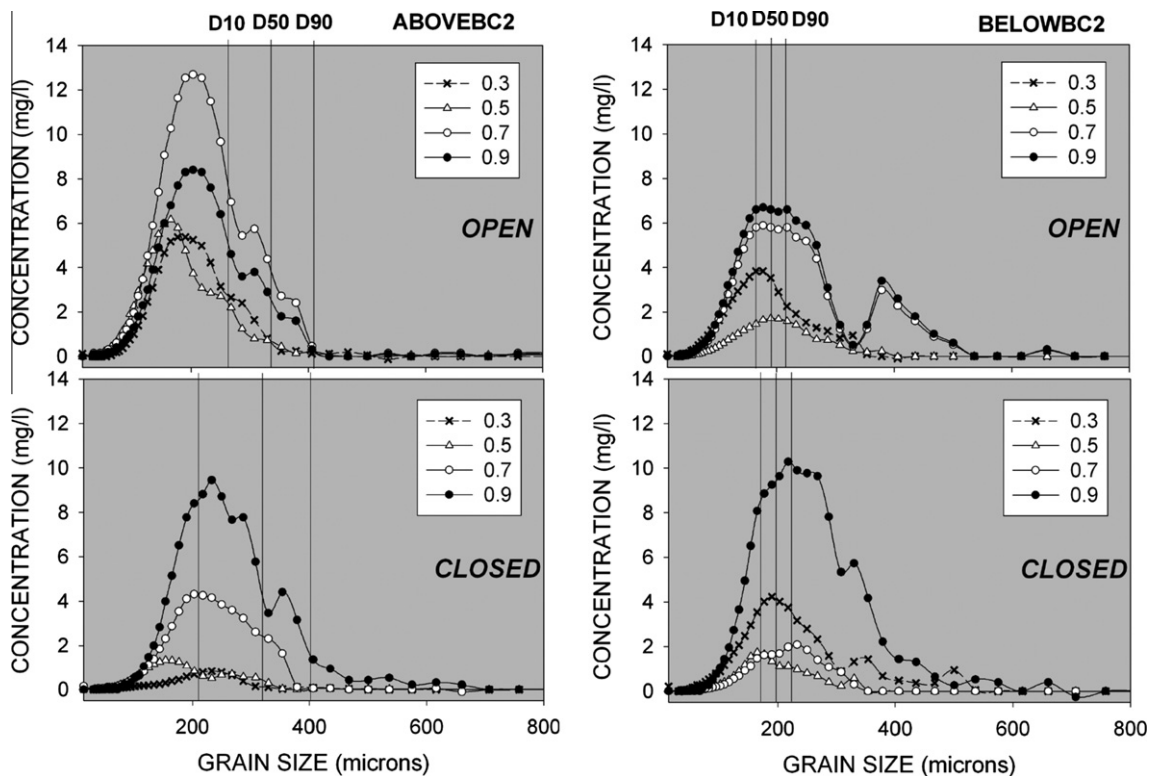

Fig. 7. Detailed grain size concentration of the suspended sand fraction (in mg/l) at the four sample depths (0.3, 0.5, 0.7 and 0.9 total water depth) from the bar face stations upriver of the Spillway (AboveBC2, left) and downriver of the Spillway (BelowBC2, right) while the Spillway was operating at capacity ("open", May 21–22, 2011) and post-closure ("closed", June 21–22, 2011). Vertical lines represent the median (D_{50}), 10th, and 90th percentile of the bed grain size at the site obtained from the bottom grabs.

6. Discussion

6.1. Channel shoaling and modulation of sediment transport

The bathymetric change analysis in Table 2 indicates that there was total channel bed storage of 9.1 million tons of sediment in the 13.3 km long channel reach downriver of the Spillway during the period when the structure was in operation. Surficial grab samples and evidence of dune migration in the change maps indicate that this deposit is likely to be almost exclusively composed of sand. Two factors suggest that this sand deposit is associated with the diversion of water at the Spillway. The first is its location. While channel reach sections upriver of the Spillway display an alternating pattern of storage and erosion likely associated with lateral bar migration in the large flood, the reach below the structure is entirely shoaling, with up to 7–8 m in some locations. Further, this shoaling begins approximately halfway down the forebay entrance to the Spillway (Fig. 4b). The lip of the forebay also shows a transition at this point from erosion to net shoaling. This transition suggests that the exit of water, which was above 8000 cms from May 14th to 27th, was focused in the upriver half of the forebay entrance, and eroded the lip of the forebay as it passed out of the main channel. The reduction of stream power is defined as the loss in potential energy associated with changing water discharge and channel slope (Lane, 1955; Knighton, 1998; Biedenharn et al., 2000), and it likely began immediately downriver of where the bulk of water loss to the forebay and, ultimately, through the Spillway, was focused. A second factor that relates the deposit to this water loss is the decreasing magnitude with distance downriver of the onset of net shoaling (Table 2). While the loss in water discharge was focused at the upper forebay region, the slowing of water velocity was likely more gradual, as was its reduction in capacity for transporting sand.

Given that sand is transported in the lowermost river channel in suspension and as bedload, with both varying with stream power, how was the sand in the channel floor deposit delivered? To address this question, we follow two approaches in the following discussion: sediment transport equations and analytical. Benthic shear stress was calculated for the six stations at AboveBC and BelowBC (Fig. 3) when the Spillway was fully open and then after closure. Stationary ADCP ensemble data (thousands of individual measurements) at each station identified on Fig. 3 were averaged for the individual depth bins, and this relationship with depth was iteratively fit to the Law of the Wall to yield shear velocities ($U*$). These velocities were then converted into shear stresses (in Pa) and apportioned into the components of total shear stress associated with dune form drag and skin friction using the methods of Nelson and Smith (1989) and given the station dune aspect ratio and bed roughness (from median grain size) shown in Table 5.

Estimates of high and low shear stress (Table 5) were determined by averaging the 30 ensembles with the highest and lowest standard deviations of velocity, respectively at each station. A complete discussion of these methods can be found in Nittrouer et al. (2011b) and Ramirez (2011). The results in Table 5 indicate that the skin friction shear stress, which is the component most closely associated with the suspension and downstream suspended advection of sand, decreases from 12.7 Pa to 9.1 Pa (averaged across the channel) when the Spillway was fully open. This decrease confirms the loss of energy for transporting sand caused by the water diversion. Channel cross-section averaged shear stresses also decrease at AboveBC (3.9 Pa) and BelowBC (6.3 Pa) in the lower discharge, post-closure sampling. These average values over the period of stationary ADCP measurement (10–30 min) can only be considered a first-order estimate of sand re-suspension capability given the large positive fluctuations in skin friction shear stress (Table 5) that likely resulted from the highly turbulent eddy regime over these large bedforms.

The analytical approach involves examining the potential available sand source in the river using data from nearby monitoring stations. Bedload transport, as defined here to be the fraction that induces migration of the channel floor dunes, scales exponentially with water discharge in the lowermost Mississippi (Nittrouer et al., 2008; Allison and Meselhe, 2010; Allison et al., 2012). The bedload transport rates above and below the Spillway are compared in Fig. 9 with a best fit regression line:

$$Q_b = 234.3 \times e^{(1.604E-4*Qw)} \tag{1}$$

Eq. (1) is derived from the data collected in the lowermost river (e.g., New Orleans and downriver) from 2003 to 2010, where Q_b is the bedload transport rate associated with dune migration in tons/

Table 5
Dune characteristics and measured bottom shear stress at AboveBC and BelowBC.

Station name/date	Dune height (m)	Dune wavelength (m)	Dune aspect ratio	Bed D_{50} (μm)	Form drag shear stress (Pa)		Skin friction shear stress (Pa)	
AboveBC1 open	1.0	38.8	0.03	268	6.0	+2.9 −1.5	7.2	+3.5 −1.7
AboveBC2 open	2.0	77.8	0.03	354	15.8	+22.9 −9.6	22.2	+32.1 −13.5
AboveBC3 open	1.3	87.5	0.01	218	3.4	+28.3 −2.4	8.7	+71.8 −6.0
BelowBC1 open	0.2	8.7	0.02	354	7.6	+55.6 −4.5	6.3	+46.1 −3.8
BelowBC2 open	4.2	130	0.03	189	0.7	+4.2 −0.02	1.4	+7.8 −0.1
BelowBC3 open	1.8	130	0.01	177	6.0	+2.5 −3.4	19.6	+8.0 −11.2
AboveBC1 closed	0.1	5.2	0.02	233	3.9	+9.3 −2.0	3.6	+8.8 −1.8
AboveBC2 closed	0.3	8.2	0.04	302	9.4	+32.8 −4.5	5.7	+19.7 −2.7
AboveBC3 closed	1.1	25.0	0.04	250	3.2	+18.5 −0	2.4	+13.9 −0
BelowBC1 closed	0.4	10.8	0.04	382	9.0	+57.3 −5.7	5.4	+33.9 −3.4
BelowBC2 closed	2.9	77.8	0.04	203	7.1	+10.5 −3.3	9.5	+14.1 −4.4
BelowBC3 closed	2.8	100	0.03	205	2.3	+5.1 −0	4.1	+8.9 −0

d and Q_w is the water discharge in m^3/s. Applying Eq. (1) to the daily water discharge at Baton Rouge and Belle Chasse, which are the nearest daily monitoring stations upriver and downriver of the Spillway), allows for a predicted daily bedload sand flux. Integrated daily over the 42 day period the Spillway was open yields a bedload flux of 4.0×10^6 tons at Baton Rouge and 1.4×10^6 tons at Belle Chasse. The differential (2.6 million tons) at these two stations is an indication of the reduced bedload transport capacity of the river with the loss of water at Bonnet Carré.

The bedload differential prediction is based on the data from New Orleans to the Gulf reach, as collected by previous studies from 2003 to 2010. When the data from three Bonnet Carré study sites are plotted on this regression (Fig. 9), the bedload flux rates from AboveBC fall on the line of previous data, while flux rates from the deposit area (BelowBC and Luling) have a much higher value than the predicted bedload flux rate. Evident from bottom grab data (Table 3), the two shallower stations at BelowBC centered over the channel deposit are much finer (mean grain size of 171–199 µm) at maximum opening and immediately after closure than the other four stations (mean grain size of 225–438 µm). This distinct bed grain size suggests that the deposit is composed mainly of fine sand, of which the shear stress to initiate grain motion and downstream-vector grain velocity is likely significantly lower than the medium sands which characterize the lowermost Mississippi River (including the AboveBC lateral bar). This finer grain size would allow for more rapid dune translation at a given discharge. For example, a line fitted to the BelowBC/Luling data in Fig. 9 would yield a significantly higher bedload daily mass flux. This grain size-induced difference may also explain why, despite the reduced water discharge, the bedload fluxes are higher at BelowBC than at AboveBC (Fig. 5) when the Spillway was operating at capacity.

The fact that the bedload flux differential between Baton Rouge and Belle Chasse (2.6 million tons) equates with only 29% of the calculated channel deposit mass suggests that sand delivery from suspension may have played a dominant role in its formation. Evidence that the bulk of the fine sand at the depocenter arrived transported as suspension includes the fact that suspended sand flux dropped by 54% between AboveBC and BelowBC (Fig. 5) when the Spillway was operating at full capacity on May 21–22nd. This differential (148,375 tons/d) is significantly higher than the 83,000 tons/d predicted for the Baton Rouge/Belle Chasse differential on that day and suggests boat-measured suspended sand flux

can vary significantly from reach-to-reach in a given discharge. The sand in suspension at AboveBC and BelowBC, when the Spillway was both open and closed (Fig. 7) is also similar in grain size to the surficial bed sand in the (median grain size of approximately 195 µm) in the depocenter immediately downriver of the structure exit point. Suspended sand increases in both concentration and median grain size as it approaches the bottom.

Following the analytical approach to estimate suspended sand availability, there is a differential between ratings curve-derived suspended sand flux at Baton Rouge and Belle Chasse: total suspended sand flux from the May 9 to June 19 opening was 12.0×10^6 tons at Baton Rouge and 6.7×10^6 tons at Belle Chasse, yielding a differential transport capacity of 5.3×10^6 tons. As Fig. 8 shows, these ratings curve-derived daily fluxes are in reasonable agreement with boat data collected at those USGS stations and from the present study.

Combining suspended and bedload flux over the 42 day event (suspended loads from Fig. 8, bedload calculated using Eq. (1)) gives 16.0×10^6 tons upriver of the Spillway (Baton Rouge) and 8.1×10^6 tons downriver at Belle Chasse. The differential (7.9 million tons) is comparable to the size of the river channel deposit (9.1 million tons). Depth profiles of suspended sand concentrations (Fig. 6) suggest a strong inter-connection with the underlying bed. Mud fractions are vertically homogenized, indicating that this is wash-load delivered from the basin, while sands show a Rouse profile (Rouse, 1937) of increasing sand content (Fig. 6) and grain size (Fig. 7) closer to the bed. Bed sand (e.g., bed-material load; Gomez, 1991) transitioning to suspension should be most active at the highest observed water discharges (i.e., downstream velocities). The highest suspended sand fluxes are observed at the highest water discharges above the Spillway when it was open to capacity (Fig. 5). Given that these observations indicate that sand in transport in the lowermost Mississippi River is derived from the underlying bed and has relatively short annual downstream migration distances (Ramirez, 2011), suspended + bedload differential between Baton Rouge and Belle Chasse cannot be thought of as a "loss term" of material passing through this reach. Instead, it reflects a reduction in the sand transport capacity due to the ~20% reduction in water discharge between the two stations due to flow into the Spillway. One complication in this comparison is that suspended sand loads at Baton Rouge exceed those at Belle Chasse even when the Spillway is closed (Fig. 8). Allison et al. (2012) attribute this difference to reduced stream power associated with
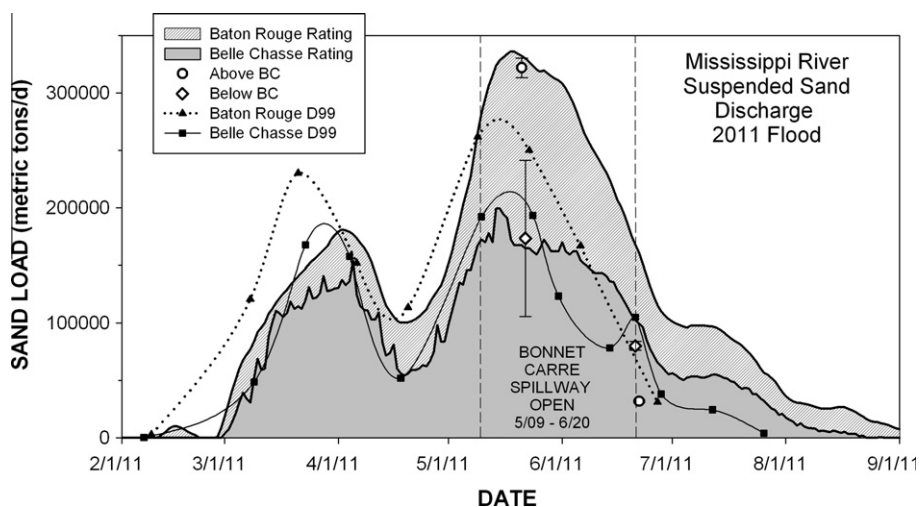

Fig. 8. Rating curve-derived suspended sand loads from the USGS monitoring stations upriver of the Spillway (Baton Rouge, darker shade) and downriver of the Spillway (Belle Chasse, lighter shade) during the 2011 flood event. Also shown are the boat-based sand flux measurements made by the USGS (using D99 depth integrative sampler) at Baton Rouge and Belle Chasse during this period, and from the present study at AboveBC and BelowBC.

declining water surface slopes approaching the Gulf of Mexico, and the periodic re-introduction of sand dredged from the Port of Baton Rouge to a point in the river immediately adjacent to the USGS monitoring site.

In addition to the aggradation of the channel deposit, sand was also being lost (1) through the Spillway, and (2) to possible deposition in the shallow forebay that was not mapped in the multibeam surveys. It is difficult to quantify export through the Spillway using the USGS daily monitoring at Airline Highway. Allison and Meselhe (2010) have shown from data collected in a previous opening (1997) that much of the sand passing through the structure is deposited in the initial ~1 km downstream of the structure and upstream of the Airline Highway USGS monitoring site. Integrating the water and sediment flux in the 31 day event in 1997 yields a sand flux into the Spillway of 2.9×10^6 tons for 1.1×10^{10} m³ total water volume. In comparison, the 2011 event passed a total of 2.14×10^{10} m³ of water. It should be noted that some of the sand flux in the Spillway in 2011 (Nittrouer et al., 2012a) might be from sand stored prior to the flood in the forebay region and remobilized during the flood, rather than directly sourced from the channel suspended + bedload flux. In the 2008 and 2011 flood events, the USGS collected data only at Airline Highway, and discontinued the measurements at the Spillway and the Interstate-10 bridge, so the sand flux into the Spillway was not directly measured.

Regardless of the incomplete nature of the sand budget derived from this analytical approach, a mass approaching the total sand flux of 16.0×10^6 tons upriver of the Spillway, rather than the differential flux caused by water loss (7.9×10^6 tons), is likely needed to account for the combined mass of the channel + Spillway + forebay deposit. This magnitude of sand capture is unlikely and it further evidence for higher flux rates in the reach opposite the Spillway than at Baton Rouge.

Observational data collected in the present study suggest the river bed morphology was in a state of disequilibrium in this enormous flood. Bedload fluxes were observed to have "excess" erosion (maximum offset at AboveBC) during the sampling (Fig. 5). This bedload flux offset suggests that the bar surfaces are deflating by transitioning sand to suspension while bedforms are translating downstream, giving a higher erosion (dune migration + bar deflation) than accretion value (dune migration only). This lateral bar deflation integrated throughout the entire Spillway opening event can also be observed in the bathymetric change map (Fig. 4a; segments A and C). Immediately after closure, the erosion–accretion offset is not observed at AboveBC and Luling, and is less pronounced in the finer grained sand at BelowBC. The downstream edge of lateral bars at segment D and H also show net accretion (Fig. 4b) that may be related to a re-deposition of sand sourced from the bar section associated with the large dune section of the field. These dunes generate additional bottom shear stress (e.g., form drag) to entrain bed material sand. The fact that the deflation observed in segments A and C was replaced after the 2012 flood, and much of the deposition at the bar downstream edges was removed (Fig. 4c), is an indication that the bars in this stabilized channel rapidly return to a positional equilibrium following an extreme flood. This also gives evidence to the local spatial variability in flux rates that can influence the sand load passed through the Spillway and deposited by the reduced energy in the channel.

Taking into account the relatively small number of measurements of energy conditions during the event in the vicinity of the Spillway water removal reach, a more complete understanding of the sand dynamics on the bar surface and how the removal of water at Bonnet Carré altered this dynamic, can only be achieved using a multi-dimensional numerical simulation of hydrodynamics and sediment transport calibrated using existing observational
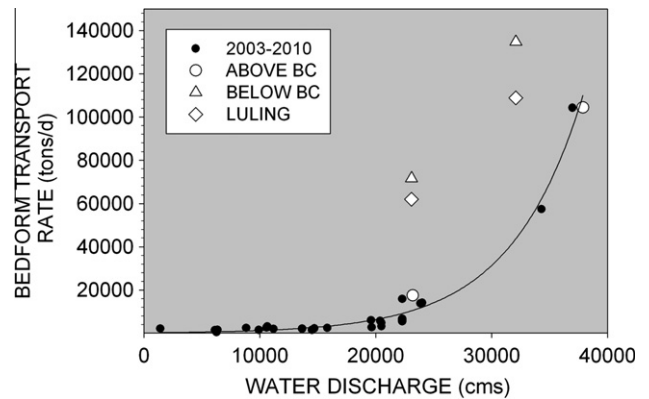

Fig. 9. Data points and best fit exponential regression line from published studies for the 2003–2010 bedload flux data for the Mississippi River in the reach from New Orleans to the Gulf, compared with measurements made upriver (AboveBC) and downriver (BelowBC, Luling) of the Spillway during the 2011 flood event.

data. These simulations are presently being carried out by the authors.

6.2. Implications for river diversion design and operation

The approximately 9.1 million tons of sand deposited downstream of the Bonnet Carré Spillway during its 42 days of operation (28 days at full capacity) is equivalent to 43% of the total suspended and bedload sand load passing the station at Belle Chasse in flood year 2011. While this flood event was unusual in magnitude, these results do suggest that rapid downstream shoaling, as a result of the reduction in stream power associated with the withdrawal of water, has major implications, in terms of percentage of overall water flow, for the use of large water diversions in river control works. The results from Bonnet Carré in 2011 suggest this channel shoaling is primarily a near-range phenomenon: 72% of the total sand storage measured downstream of the Spillway in May–June 2011 (segments F to I in Fig. 4a) was in the closest channel reach (3.7 km long segment F). This storage decreased rapidly: 15% in segment G, 7.5% in H and 5.5% in segment I. The rapid decrease suggests that the channel re-establishes equilibrium (e.g., no channel aggradation) further downstream. Elevated suspended sand concentrations at BelowBC in June 2011 was likely early evidence of the reworking of this deposit that was observed in the June 2012 survey (Fig. 4c). The latter results show that 69% of the sand deposited in segments F–I (6.3×10^6 tons) was removed in the subsequent flood year. The trend, however, is not tied to volume of deposition on a segment-by-segment basis: segments G and H had net deposition between June 2011 and June 2012 (Fig. 4c). This trend suggests that some sand was removed from the study reach by suspended and bedload transport, while a percentage translated out of segment F only was transported downstream as far as segments G and H.

In the Mississippi River in Louisiana, the State of Louisiana's 2012 Master Plan draft for coastal restoration (LACPRA, 2012) provides a blueprint for action over the next 50 years. Three large water and sediment diversions are envisioned for the river channel downriver of Belle Chasse to divert sediment into adjacent shallow estuarine areas for wetland creation and maintenance. These would be operated at full capacity (50,000 cfs or 1416 cms) at river discharges above 600,000 cfs (16,990 cms). A fourth diversion in the same reach (Upper Breton Diversion) would operate at the same capacity with river flows of 600,000–900,000 cfs (25,485 cms). Discharges above that limit would operate at 250,000 cfs (7079 cms), and are equivalent to the rated water discharge of the Bonnet Carré Spillway. Since these diversions are

planned to operate annually, including 8% of each river flow at discharges between 200,000 and 600,000 cfs (5663–16,990 cms), the downstream shoaling inferred from the 2011 flood data has major implications for maintaining navigability of deep draft vessels in the river.

Several caveats are apparent in this statement. First, if this deposit is reworked during intervals when the diversions were not operated, as was observed in the June 2012 remapping of the depositional reach, this would limit the shoaling risk. Second, the Bonnet Carré Spillway is a flood-control structure and was not designed to maximize the diversion of sediment, particularly sand. The decantation of sand-poor surface water (Fig. 6) that is characteristic of this structure would tend to maximize the ratio of the loss of stream power (water) to the removal of suspended sediment. Deeper diversions designed to draw water from greater water depths might reduce the magnitude of sand settling downchannel of the withdrawal point. Finally, the location of the diversion in terms of distance upriver from the Gulf of Mexico, will also likely play a role in shoaling magnitude. Bonnet Carré is above the estuarine reach and above all but a minor tidal modulation of stream velocities (Galler and Allison, 2008). A reduction in hydraulic head might also be expected further downstream (Allison et al., 2012; Nittrouer et al., 2012b), which might reduce the suspended sand load reaching reaches closer to the Gulf. In summary, these caveats suggest that the data from Bonnet Carré may be most valuable for numerically modeling diversion designs to improve sand capture efficiency, and to minimize near-range channel shoaling downriver of the structure.

The operation of diversions equal in scale to that of the Bonnet Carré Spillway for land building can be designed to take advantage of near-range shoaling. By regular dredging and pipeline conveyance of sand through the diversion, which creates an "augmented diversion" (Allison and Meselhe, 2010), the sediment to water ratio of diverted water can be increased to maximize land building potential. The operation may involve either the direct injection of dredged sand into the active flow through the diversion or the stockpiling of sand in the exit channel while the diversion is closed (to re-mobilize when it opens). It may also increase the cost:benefit ratio of financial decision-making to determine whether a particular diversion is constructed. An example includes offsetting the expensive maintenance dredging that may be required to maintain a navigable deep draft channel through the reach for shipping.

7. Conclusions

The results of this study lead to the following conclusions:

(1) The water diversion associated with the 42-day opening of the Bonnet Carré Spillway in the Mississippi River in May–June 2011 resulted in a reduction of stream power in the main channel and led to rapid aggradation of a sand deposit immediately downriver of the exit point. The mass of this sand deposit is calculated to be approximately 9.1 million tons. The deposit extends throughout the 13 km long river reach surveyed downriver of the Spillway entrance and decreases rapidly and progressively in magnitude downriver. Approximately 69% of this stored sand in the channel was removed after closure by the subsequent flood in 2012.

(2) The channel deposit is composed of fine sand (at least near the surface). A sediment budget analytical approach by using bedload and suspended load fluxes measured in the present study upriver and downriver of the Spillway and at nearby monitoring stations cannot account for the entire mass of this deposit, much less additional sand loss through the

Spillway itself. However, sand delivery from suspension appears to be the main mechanism associated with the deposit's formation. This assumption is based on the equivalent size of sand in samples from the lower water column and surficial samples from the deposit, which is finer than on the lateral channel bars upriver of the Spillway entrance. This suggests a link between observed bar deflation and increased sand concentration in the lower water column of the river channel. This also implies that fluxes of sand in suspension measured in the lower Mississippi River are highly spatially variable, as they derive from reach-scale hydrodynamics.

(3) The limited sediment transport data collected for calculating bottom shear stresses in the present study does show a reduction in bottom shear stress, which indicates the necessary energy to maintain sand in suspension downriver of the Spillway relative to upriver measurements. Ongoing multidimensional modeling calibrated using the water and sediment transport data presented in this study will be necessary to better understand the hydrodynamic conditions that led to deposit formation.

(4) The present study supplements the limited quantitative observations of the effects of a large water diversion on sediment dynamics in large rivers. This information is critical for the Mississippi delta, since large water and sediment diversions from the river channel are presently under consideration for restoring coastal wetlands. The degree of shoaling likely associated with annual operation (as opposed to Bonnet Carré Spillway, which is only operated in extreme floods) is a major consideration in rivers that use the channel as a deep-draft transportation artery for shipping.

References

Allison, M.A., Meselhe, E.A., 2010. The use of large water and sediment diversions in the lower Mississippi River (Louisiana) for coastal restoration. J. Hydrol. 387, 346–360.

Allison, M.A., Demas, C.R., Ebersole, B.A., Kleiss, B.A., Little, C.D., Meselhe, E.A., Powell, N.J., Pratt, T.C., Vosburg, B.M., 2012. A water and sediment budget for the lower Mississippi–Atchafalaya River in flood years 2008–2010: implications for sediment discharge to the oceans and coastal restoration in Louisiana. J. Hydrol. 432 (3), 84–97.

Biedenharn, D.S., Thorne, C.R., Watson, C.C., 2000. Recent morphological evolution of the Lower Mississippi River, USA. Regul. Rivers: Res. Manage. 13, 517–536.

Edwards, T.K., Glysson, G.D., 1988. Field Methods for Measurement of Fluvial Sediment. US Geological Survey Open-File, Report 86-531.

Gomez, B., 1991. Bedload transport. Earth Sci. Rev. 31, 89–132.

Knighton, D., 1998. Fluvial Forms and Processes. John Wiley & Sons, New York, NY.

LACPRA, 2012. Louisiana's Comprehensive Master Plan for a Sustainable Coast. Published by the Lousisiana Coastal Protection and Restoration Authority (LACPRA), State of Louisiana, Baton Rouge, LA, 170 pp.

Lane, E.W., 1955. The importance of fluvial morphology in hydraulic engineering. Proc. Am. Philos. Soc. 123, 168–202.

Miao, C., Ni, J., Borthwick, A.G.L., Yang, L., 2011. A preliminary estimate of human and natural contributions to the changes in water discharge and sediment load in the Yellow River. Global Planet. Change 76, 196–205.

Mirza, M.M.Q., 1998. Diversion of the Ganges water at Farakka and its effects on salinity in Bangladesh. Environ. Manage. 22, 711–722.

Nelson, J.M., Smith, J.D., 1989. Flow in meandering channels with natural topography. In: Ikeda, S., Parker, G. (Eds.), River Meandering, pp. 69–102.

Nittrouer, J.A., Allison, M.A., Campanella, R., 2008. Evaluation of bedload transport in the lower Mississippi River: implications for sand transport to the Gulf of

Mexico. J. Geophys. Res. – Earth Surf. Processes 113, F03004. http://dx.doi.org/10.1029/ 2007JF000795.

Nittrouer, J.A., Mohrig, D., Allison, M.A., Peyret, A.B., 2011a. The lowermost Mississippi River: a mixed bedrock-alluvial channel. Sedimentology. http://dx.doi.org/10.1111/j.1365-3091.2011.01245.

Nittrouer, J.A., Mohrig, D., Allison, M.A., 2011b. Punctuated sand transport in the lowermost Mississippi River. J. Geophys. Res. – Earth Surf. Processes 116, F04025. http://dx.doi.org/10.1029/2011JF002026.

Nittrouer, J.A., Best, J.L., Brantley, C., Cash, R.W., Czapiga, M., Kumar, P., Parker, G., 2012a. Mitigating land loss in coastal Louisiana by controlled diversion of Mississippi River sand. Nat. Geosci. 5, 534–537.

Nittrouer, J.A., Shaw, J., Lamb, M.P., Mohrig, D., 2012b. Spatial and temporal trends for water-flow velocity and bed-material sediment transport in the lower Mississippi River. Geol. Soc. Am. Bull.. http://dx.doi.org/10.1130/B30497.1.

Ramirez, M.T., 2011. Suspension of Bed Material over Lateral Sand Bars in the Lower Mississippi River, Southeastern Louisiana, M.S. Thesis, University of Texas at Austin, 120 p.

Rouse, H., 1937. Modern conceptions of the mechanics of fluid turbulence. Trans. Am. Soc. Civ. Eng. 102, 463–543.

Saucier, R.T., 1994. Geomorphology and Quaternary Geologic History of the Lower Mississippi Valley. U.S. Army Corps of Engineers, Mississippi River Commission, Vicksburg, MS, vol. 1, 364 p.

Smith, S.E., Büttner, G., Szilagy, I.F., Horvath, L., Aufmuth, J., 2000. Environmental impacts of river diversion: Gabcikovo Barrage system. J. Water Resour. Plann. Manage. 126, 138–145.